Zeitschrift: Bulletin des Schweizerischen Elektrotechnischen Vereins

Herausgeber: Schweizerischer Elektrotechnischer Verein ; Verband Schweizerischer Elektrizitätswerke

Band: 51 (1960)

Heft: 20

Artikel: Potential Distribution Above A Serrated Cathode

Autor: Weber, E.

DOI: https://doi.org/10.5169/seals-917067

Potential Distribution Above A Serrated Cathode

By *E. Weber*, New York

621.3.032.21:621.319.7

In certain applications it is desired to employ a cathode surface of the serrated type as shown in Fig. 1. The potential distribution above the surface will be periodic in the same manner as the cathode surface and will approximate parallel planes at a certain height h which is determined by the degree of undulation that one might tolerate.

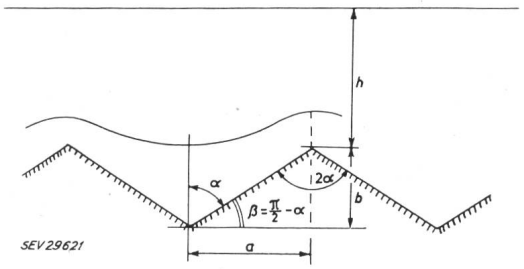

Fig. 1

Serrated Cathode Surface

a Half period of serration; *b* Depth of serration; *h* Height above the serrated cathode where the equipotential lines are parallel and show undulation smaller than tolerable; β Serration angle

To find the potential distribution, we shall use the method of conformal mapping and select for this purpose an elemental strip of the periodic field structure as shown in Fig. 2a. The linear section *1—2* is an elemental part of the cathode surface, an equipotential surface; and the lines *2—3′* and *3″—1* represent the singular field lines emanating from the singular points *2* and *1* of the cathode surface,

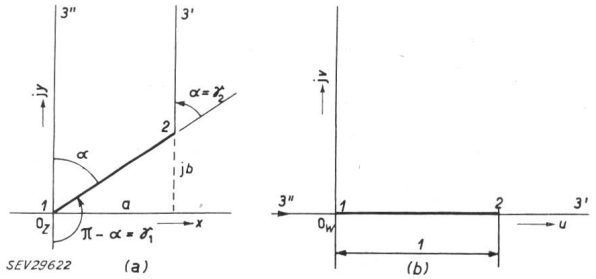

Fig. 2

Mapping into the upper Half-plane

(*a*) *z*-plane: *a* Half periode of serration; j*y* Imaginary part of complex variable *z*; *x* Real part of complex variable *z*; j*b* Depth of serration in the complex *z*-plane

(*b*) *w*-plane; j*v* Imaginary part of complex variable *w*; *u* Real part of complex variable *w*

respectively. Placing the origin of the complex *z*-plane into point *1* and selecting its image in the *w*-plane again as origin, we map conformally the strip of the *z*-plane into the upper half *w*-plane Fig. 2b by means of the *Schwarz-Christoffel* mapping function [1][1]). In this case, we can even select the image of point *2* as $w_2 = 1$ because the total polygonal region has only three vertices. The correspondence of the points and mapping coefficients is now as follows:

Vertex Points $\nu =$	1	2	$3'/3''$
z_ν	$0 + j0$	$a + jb$	$\begin{cases} a + j\infty \\ 0 + j\infty \end{cases}$
w_ν	0	1	$\begin{cases} +\infty \\ -\infty \end{cases}$
γ_ν	$\pi - \alpha$	α	π
$\frac{1}{\pi} \cdot \gamma_\nu$	$1 - \frac{\alpha}{\pi}$	$\frac{\alpha}{\pi}$	1

The mapping function is thus defined by

$$\frac{dz}{dw} = N\, w^{(\alpha/\pi - 1)} (1 - w)^{-\alpha/\pi} \tag{1}$$

where we arbitrarily anticipate a standard form of integral by modifying the second factor from the conventional $(w - 1)$ and accepting the burden in the constant N. The integration leads to

$$z = N \int w^{(\alpha/\pi - 1)} (1 - w)^{-\alpha/\pi}\, dw + C \tag{2}$$

which we can identify as the incomplete Beta function of *Euler*

$$z = N \int_0^w w^{(\alpha/\pi - 1)} (1 - w)^{-\alpha/\pi}\, dw \tag{3}$$

if we take advantage of the correspondence of the origins in the *z*- and *w*-planes.

The constant N is readily found by establishing the correspondence of the second vertex z_2 to $w = 1$, namely

$$z_2 = a + jb = N \int_0^1 w^{(\alpha/\pi - 1)} (1 - w)^{-\alpha/\pi}\, dw = N\, B\left(\frac{\alpha}{\pi}, 1 - \frac{\alpha}{\pi}\right) \tag{4}$$

where now the definite integral is the standard Beta function of Euler [2; 3], also defined by

$$B\left(\frac{\alpha}{\pi}, 1 - \frac{\alpha}{\pi}\right) = \frac{\Gamma\left(\frac{\alpha}{\pi}\right) \Gamma\left(1 - \frac{\alpha}{\pi}\right)}{\Gamma(1)} = \frac{\pi}{\sin \alpha} \tag{5}$$

if we utilize the recurrence formula for the Gamma function

$$\Gamma(x)\, \Gamma(1 - x) = \frac{\pi}{\sin \pi x}$$

The constant N is thus from Eqns. (4) and (5)

$$N = \frac{\sin \alpha}{\pi} (a + jb) \tag{6}$$

and we obtain the final solution for the mapping relation

$$z = \frac{\sin \alpha}{\pi} (a + jb)\, B\left(\frac{\alpha}{\pi}, 1 - \frac{\alpha}{\pi}, w\right) \tag{7}$$

essentially a special form of the incomplete Beta function because of the interrelationship between the parameters.

For the numerical computation one must resort to appropriate series expansions. The simple linear transformation

$$w = \frac{t}{1 + t}, \qquad t = \frac{w}{1 - w}$$
$$dw = \frac{dt}{(1 + t)^2} \tag{8}$$

renders Eq. (3) in the form

$$z = N \int_0^t t^{\alpha/\pi - 1} \frac{dt}{1 + t} \tag{9}$$

[1]) Refer to the Bibliography at the end of the article.

which, for $|t|<1$, permits binominal expansion of the second factor. Since the integrand is analytical for $|t|<1$ except at $t=0$ which point must be excluded in any case because it corresponds to $w=0$, a vertex, we can integrate term by term and obtain the final form

$$z = N t^{\mu}\left[\frac{1}{\mu} - \frac{t}{1+\mu} + \frac{t^2}{2+\mu} - \frac{t^3}{3+\mu} + \ldots\right] \cdot |t|<1 \qquad (10)$$

$$\mu = \frac{\alpha}{\pi} < \frac{1}{2}$$

From Eq. (8) we identify $|t|<1$ as equivalent to

$$|w|<|w-1|, \quad \text{or} \quad \mathrm{Re}\,|w|<1/2 \qquad (11)$$

To obtain a solution valid for $|t|>1$, we integrate from z_2 as reference point, which leads to

$$\int_{z_2}^{z} \mathrm{d}z = z - z_2 = N \int_{w=1}^{w} w^{(\alpha/\pi-1)}\,(1-w)^{-\alpha/\pi}\,\mathrm{d}w$$

With z_2 from Eqns. (4) and (5), and the same linear transformation of Eq. (8) we have

$$z = N\left[\frac{\pi}{\sin\alpha} + \int_{\infty}^{t} t^{\alpha/\pi-2}\,\frac{\mathrm{d}t}{1+1/t}\right] \qquad (12)$$

The integrand is the same as in Eq. (9) except that we divided numerator and denominator by t in order to now permit expansion of the second factor for $|t|>1$. Again, the integrand is analytical except at $t=\infty$ which point must be excluded in any case because it corresponds to $w=1$, a vertex. Integrating then term by term we obtain the final form

$$z = N\left\{\frac{\pi}{\sin\alpha} - t^{\mu}\left[\frac{1}{(1-\mu)\,t} - \frac{1}{(2-\mu)\,t^2} + \frac{1}{(3-\mu)\,t^3} - + \ldots\right]\right\} \qquad (13)$$

where

$$|t|>1 \text{ and } \mu = \frac{\alpha}{\pi} < 1/2$$

which is valid for $\mathrm{Re}\,|w|>1/2$. Both series expansions converge rather rapidly close to the vertices of the polygonal region.

Having established the complete mapping relationship between z and w (or t) planes, we must now solve for the potential distribution in the w-plane. The complex potential function describing the field surrounding the finite plane strip 1—2 is given by [1] p. 340, see also p. 298.

$$P = \frac{\lambda}{2\pi\varepsilon}\cosh^{-1}(2w-1) = \Phi + \mathrm{j}\,\psi \qquad (14)$$

where Φ is the electrostatic potential and ψ the flux function. The equipotential surfaces are the family of confocal ellipses with points *1* and *2* as foci; the flux lines or field lines are the orthogonal family of confocal hyperbolae. The center of the geometry is $w=u=1/2$. Inversion of Eq. (14) and separation of real and imaginary parts gives

$$2u-1 = \cosh\Phi'\cos\psi' \qquad (15)$$
$$2v = \sinh\Phi'\sin\psi'$$

where the factor $2\pi\varepsilon/\lambda$ was absorbed in the field functions as indicated by the primes. If we put $\Phi'=0$, we must conclude from Eq. (15)

$$v=0, \quad 2u-1=\cos\psi'$$

so that $0<u<1$ in order to give real values of ψ'; this is then the strip of potential value zero. Should we want to ascribe any arbitrary potential value Φ_0 to this strip, then we need to add this constant to Eq. (14). The charge value λ per unit depth collected on the strip must be known, since we have a single electrode surface.

We can eliminate ψ' from Eq. (15) by use of the identity $\cos^2\psi' + \sin^2\psi' = 1$, and thus have

$$\left(\frac{2u-1}{\cosh\Phi'}\right)^2 + \left(\frac{2v}{\sinh\Phi'}\right)^2 = 1 \qquad (16)$$

the equation of the ellipses, where the major axis $2A = \cosh\Phi'$ and the minor axis $2B = \sinh\Phi'$ as in Fig. 3b. Assuming different values of Φ', Eq. (16) defines individual ellipses, giving the correlated values u and v and thus permitting the transferrance to the z-plane by either Eq. (10) or (13), depending on $u = \mathrm{Re}\,|w| \gtrless 1/2$.

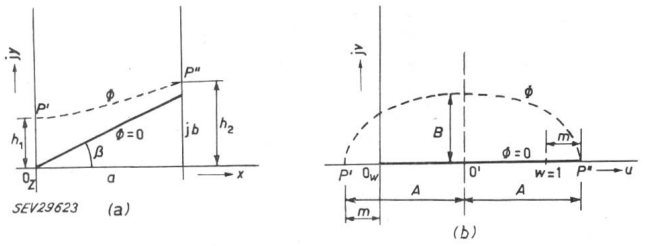

Fig. 3

Correspondence of Equipotential Surfaces

(*a*) z-plane: Φ Electrostatic potential; h_1, h_2 Height of points P' and P'' respectively on the equipotential Φ above the reference plane

(*b*) w-plane: *2A* Major axis of the equipotential ellipses; *2B* Minor axis of the equipotential ellipses; m Distance of images of points P' and P'' respectively from the vertices O_w and $w=1$ respectively

Of greatest interest is generally the rapidity with which the undulation of the equipotential surfaces subsides, i. e. how rapidly the heights of the extreme points h_1 and h_2 in Fig. 3a become nearly equal. Inasmuch as the images of the points P' and P'' lie along the real axis of the u-plane, and in fact at equal distances m from the vertices, we need only consider the real values

$$u' = -m, \qquad u'' = 1+m$$
$$t' = \frac{-m}{1+m}, \qquad t'' = \frac{1+m}{-m} = -M = \frac{1}{t'} \qquad (17)$$

as the values to be used, respectively, in (10) for h_1 and in Eq. (13) for h_2. If we also observe

$$a + \mathrm{j}b = \sqrt{a^2+b^2}\;\mathrm{e}^{\mathrm{j}(\pi/2-\alpha)}$$

we can write Eq. (6)

$$N = \frac{1}{\pi}\sqrt{a^2+b^2}\cdot\sin\alpha\cdot\mathrm{e}^{\mathrm{j}(\pi/2-\alpha)} = \mathrm{j}\,\frac{a}{\pi}\,\mathrm{e}^{-\mathrm{j}\alpha} \qquad (18)$$

Introducing t' from Eqns. (17) into (10), we have

$$z' = \mathrm{j}h_1 = \mathrm{j}\,\frac{a}{\pi}\,M^{-\mu}\left[\frac{1}{\mu} + \frac{M^{-1}}{1+\mu} + \frac{M^{-2}}{2+\mu} + \frac{M^{-3}}{3+\mu} + \ldots\right] \qquad (19)$$

for the computation of h_1 for various values of m. Similarly, we can bring Eq. (13) into the form

$$z'' = a + \mathrm{j}h_2 = a + \mathrm{j}b + \frac{a}{\pi}\,M^{\mu}\left[\frac{M^{-1}}{1-\mu} + \frac{M^{-2}}{2-\mu} + \frac{M^{-3}}{3-\mu} + \ldots\right] \qquad (20)$$

for the computation of h_2 for the same values of m. Fig. 4

gives the results of these computations against the angle β of the serration. As m increases, the significant level difference $h_2 - h_1$ decreases as one must expect. This undula-

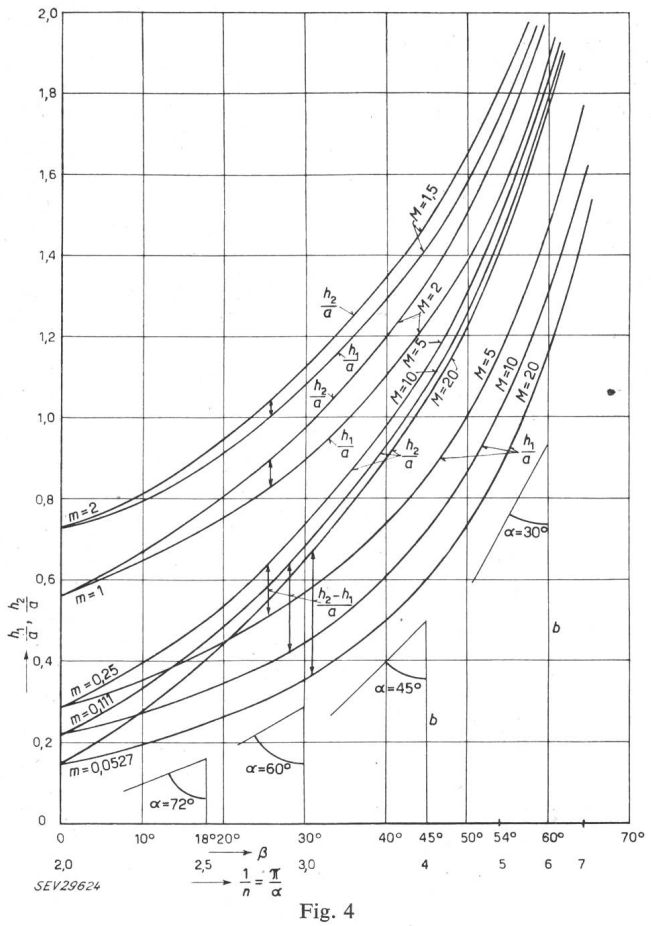

Fig. 4

Evaluation of Eq. [19] and [20] as a function of β

β Angle of serration; $\alpha = \pi/2 - \beta$; h_1 Height of P' above reference plane; h_2 Height of P'' above reference plane; a Half period of serration; m Distance of images of points P' and P'' from vertices;

$$M = \frac{1 + m}{m}$$

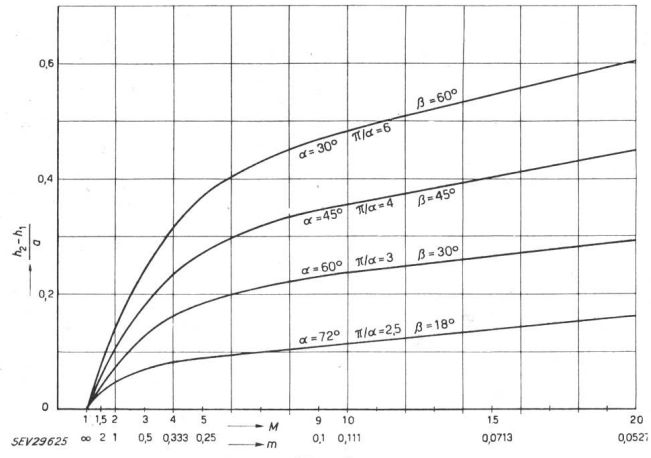

Fig. 5

Ondulation of $(h_2 - h_1)/a$ with M

$(h_2 - h_1)/a$ Measure of undulation (relative undulation); a Half period of serration; m Distance of images of points P' and P'' from vertices; $M = \dfrac{1 + m}{m}$

tion measure $(h_2 - h_1)/a$ is also plotted in Fig. 5, directly against M and Fig. 6 gives the most important section with enlarged scales to permit more accurate interpolation for larger values of m.

We can now pose the question: At which height above the base plane $y = 0$ will the undulation have decreased to a selected small percentage of the half-period a of the

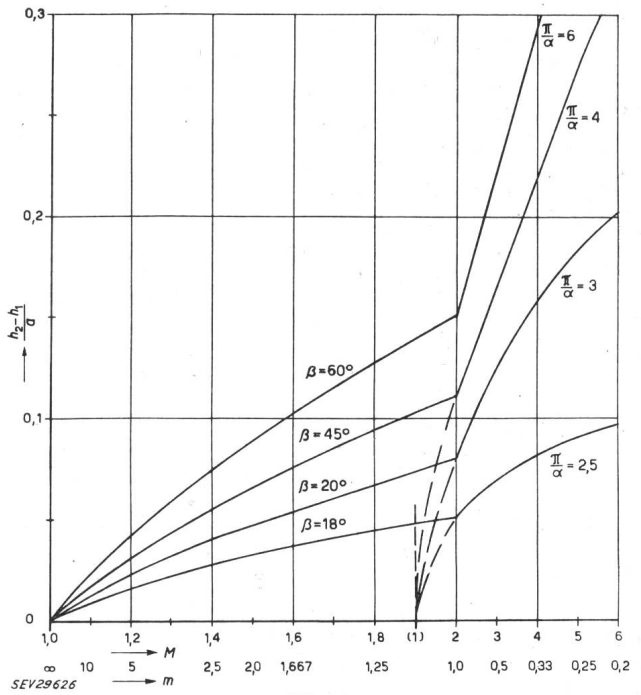

Fig. 6

Enlarged Picture of Fig. 5 for small values of M

serrated cathode. For this purpose Fig. 7 has been prepared in which the distances h_1/a and h_2/a are plotted against the difference $(h_2 - h_1)/a$. Selecting a value of 10% or $(h_2 - h_1)/a = 0.10$, we find that $h_2/a = 1.36$ for the angle $\alpha =$

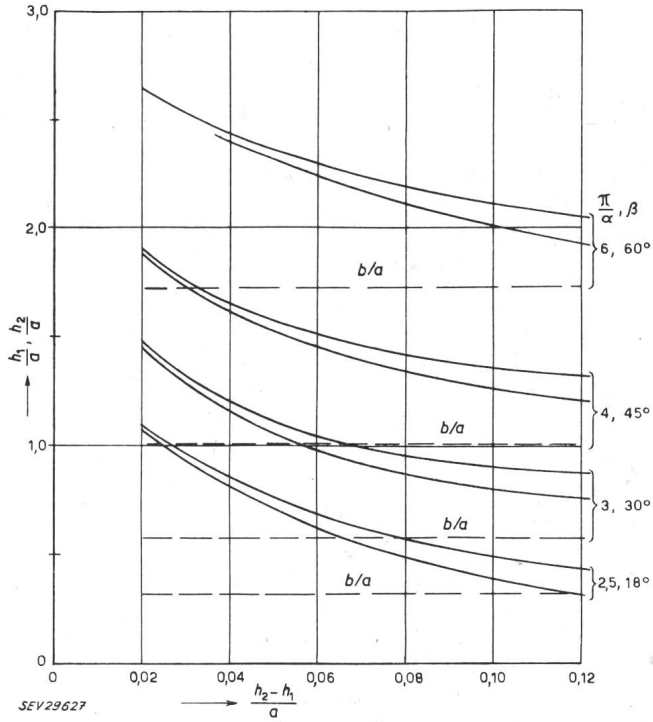

Fig. 7

h_1/a and h_2/a as functions of the relative undulation $(h_2 - h_1)/a$

$\beta = 45°$, or that we must stay at a height of $0.36a$ above the tips of the serration. Since the latter measure might be considered most significant, the dotted lines in Fig. 7 repre-

sent the values b/a, i. e. the level of the peaks of the serration. The smaller the desired undulation, the larger must be the distance above the serration peaks. For a maximum undulation of 2%, the necessary distance above the peaks is of the same order as the half period a, varying in fact from $0.775a$ for $\beta = 18°$ ($\pi/\alpha = 2.5$) to $0.908a$ for $\beta = 60°$ ($\pi/\alpha = 6$). This confirms the rule of thumb that the effect of local field distortions extends about the same distance as the principal geometric dimension of the field disturbing structure. The actual potential distribution for $\alpha = \beta = 45°$, or $\pi/\alpha = 4$ is shown in Fig. 8 together with the numerical values for m and the relative undulation $(h_2 - h_1)/a$.

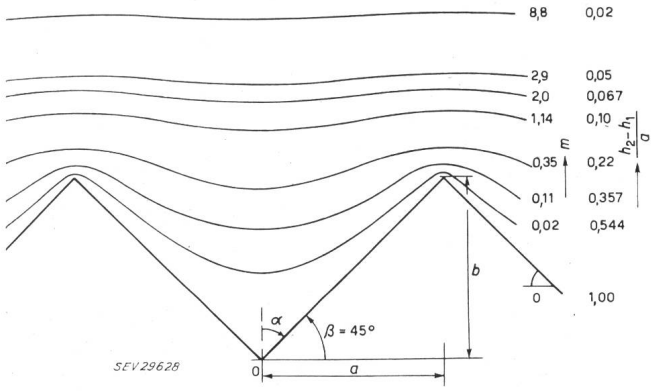

Fig. 8
Potential Distribution for $\alpha = \beta = 45°$

The field vector E is rather readily evaluated as the negative potential gradient. In the complex z-plane, we obtain the complex value of E by [1]:

$$E_z = -\left(\frac{dP}{dz}\right)^* = -\left(\frac{dP}{dw} \cdot \frac{dw}{dz}\right)^* \qquad (21)$$

where the asterisk indicates the conjugate complex number. With Eqns. (14) and (1) and the special form (18) for N, this leads to

$$E_z = -j\frac{\lambda}{2\pi\varepsilon} \cdot \frac{\pi}{a}\left(\frac{w}{w-1}\right)^{1/2-\alpha/\pi} \qquad (22)$$

Since $a/\pi \leqq 1/2$, the field vector will approach zero value as $w \to 0$, and will approach infinity as $w \to 1$, which is obviously correct from physical principles. The general forms in Eqns. (10) and (13) give the relationship between w (or t) and z, so that Eq. (22) can readily be evaluated at any point of the z-plane.

Again, it will be most instructive to compute the field strength variation along the two vertical field lines emerging at the vertices and imaged as the field line sections of the u-axis in Fig. 3b. For the left part, emanating from O_w, we have $w' = u' = -m$, so that (22) becomes

$$E_z' = -j\frac{\lambda}{2a\varepsilon}\left(\frac{m}{m+1}\right)^{1/2-\alpha/\pi} \qquad (23)$$

Thus the field vector points vertically downward in Fig. 3a as we expect it, and increases from the value zero at O_z to a fixed value

$$E_0 = -j\frac{\lambda}{2a\varepsilon} \qquad (24)$$

as $m \to \infty$. As a matter of fact, $|E_0|$ is the field strength value in the uniform field reached for all practical purposes at the equipotential line in Fig. 8 for which the undulation is of the order of 2% or less. Using Eq. (24), we get the simple expression

$$E_z'/E_0 = \left(\frac{m}{m+1}\right)^{1/2-\alpha/\pi} = M^{\alpha/\pi - 1/2} \qquad (25)$$

Its value is plotted in Fig. 9 for two angles of serration in the lower section of the graph marked *min* to indicate that actually this field line starting from the valley depth of the serration has the lowest field strength values in the entire field structure.

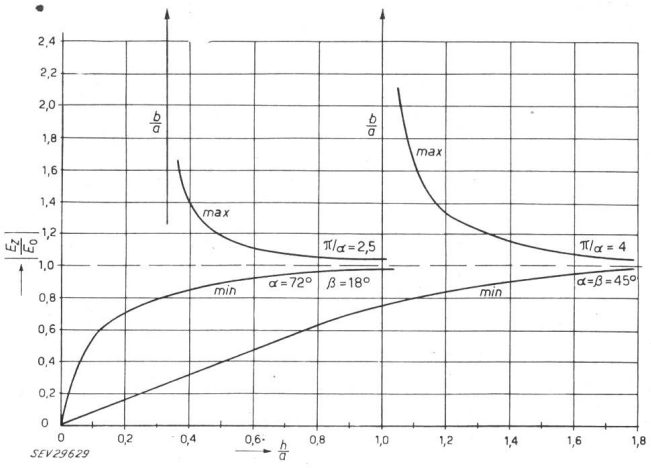

Fig. 9
Relative field strengths along maximum and minimum field lines (Plot of Eq. 25) for two angles of serration)
E Field strength

For the right field line part of the u-axis in Fig. 3b we have

$$E_z''/E_0 = \left(\frac{m+1}{m}\right)^{1/2-\alpha/\pi} = M^{1/2-\alpha/\pi} = E_0/E_z' \qquad (26)$$

the reciprocal value to Eq. (25), which characterizes it as the field line of maximum field strength values. Fig. 9 gives the values for the same two angles of serration; as we approach the location of the peaks of the serration, the field strength values will, of course, go toward infinity.

Bibliography

[1] *Weber, E.:* Electromagnetic Fields. Theory and Applications. Vol. 1: Mapping of Fields. New York: Wiley; London: Chapman & Hall 1950. Chapt. 7, Sect. 27: Conformal Mapping of Straight-Line Polygons, p. 325...362.

[2] *Jahnke, E.* and *F. Emde:* Tables of Functions. Leipzig: Teubner 1938; 3rd. Ed., reprinted by Dover, New York 1943. p. 20.

[3] *Peirce, B. O.:* A Short Table of Integrals. 4th Ed., revised by *R. M. Foster*. Boston: Ginn 1956. p. 67, No. 497; p. 95, No. 797, 798.

Author's address:
Professor *E. Weber*, Polytechnic Institute of Brooklyn, 333 Jay Street, Brooklyn 1, N. Y. (USA).